

Termination of autophagy and reformation of lysosomes regulated by mTOR

Li Yu^{1,2,3}, Christina K. McPhee^{4,5}, Lixin Zheng¹, Gonzalo A. Mardones^{6,7}, Yueguang Rong^{2,3}, Junya Peng^{2,3}, Na Mi^{2,3}, Ying Zhao⁸, Zhihua Liu¹, Fengyi Wan¹, Dale W. Hailey⁶, Viola Oorschot⁹, Judith Klumperman⁹, Eric H. Baehrecke⁴ & Michael J. Lenardo¹

Autophagy is an evolutionarily conserved process by which cytoplasmic proteins and organelles are catabolized^{1,2}. During starvation, the protein TOR (target of rapamycin), a nutrient-responsive kinase, is inhibited, and this induces autophagy. In autophagy, double-membrane autophagosomes envelop and sequester intracellular components and then fuse with lysosomes to form autolysosomes, which degrade their contents to regenerate nutrients. Current models of autophagy terminate with the degradation of the autophagosome cargo in autolysosomes^{3–5}, but the regulation of autophagy in response to nutrients and the subsequent fate of the autolysosome are poorly understood. Here we show that mTOR signalling in rat kidney cells is inhibited during initiation of autophagy, but reactivated by prolonged starvation. Reactivation of mTOR is autophagy-dependent and requires the degradation of autolysosomal products. Increased mTOR activity attenuates autophagy and generates proto-lysosomal tubules and vesicles that extrude from autolysosomes and ultimately mature into functional lysosomes, thereby restoring the full complement of lysosomes in the cell—a process we identify in multiple animal species. Thus, an evolutionarily conserved cycle in autophagy governs nutrient sensing and lysosome homeostasis during starvation.

We found that after nutrient deprivation of normal rat kidney (NRK) cells, multiple lysosomes fuse with each autophagosome. After 4 h, essentially all lysosomes were consumed into fewer and larger autolysosomes that expressed lysosomal-associated membrane protein 1 (LAMP1) (Supplementary Movie 1; Fig. 1a). However, the size and number of lysosomes had largely recovered after 12 h of starvation (validated independently with cathepsin D as a luminal marker; Fig. 1a and Supplementary Figs 1, 2). We observed similar changes *in vivo* after starvation in the lysosomes of the fat body of *Drosophila melanogaster* expressing green fluorescent protein (GFP)-tagged LAMP1 (LAMP1-GFP; Supplementary Fig. 3), and also in cell lines derived from fish, amphibians, birds and other mammals (Supplementary Fig. 4), although the kinetics varied between different cell lines. Hence, a homeostatic cycle that involves the consumption and restoration of lysosomes during starvation-induced autophagy seems to be evolutionarily conserved.

We hypothesized that a process of lysosome reformation might follow the establishment of autolysosomes. In cells starved for 8 h and expressing yellow fluorescent protein (YFP)-tagged LAMP1 (LAMP1-YFP) or stained for endogenous LAMP1, we observed tubular structures extending from autolysosomes (Fig. 1b and Supplementary Fig. 5). The membrane-limited nature of these tubules could be

appreciated by transmission electron microscopy (TEM) and immuno-TEM, which also revealed LAMP1 on the surface of the tubules but showed that they contained little or no discernible luminal content from the autolysosomes (Fig. 1c and Supplementary Figs 5, 6). Next, we used live-cell imaging to monitor serum-deprived NRK cells expressing LAMP1-YFP and cyan fluorescent protein (CFP)-tagged microtubule-associated light chain 3 (CFP-LC3). Lysosomes and autolysosomes express LAMP1 and autophagosomes and autolysosomes express LC3, so this combination allows us to distinguish between lysosomes (LAMP1⁺, LC3⁻) and autolysosomes (LAMP1⁺, LC3⁺). After 4 h of starvation, most, if not all, lysosomes coalesced into enlarged autolysosomes (Fig. 1d). After 8 h of starvation, we saw LAMP1-positive tubular structures extending from autolysosomes (Fig. 1d). After 12 h of starvation, LC3 was dispersed and less punctate than at earlier time points, indicating that autophagy had slowed and that the size and number of lysosomes, now devoid of LC3, had returned to pre-starvation levels (Fig. 1d). We saw similar LAMP1-positive tubules in different cell types from various animal species (Supplementary Fig. 4).

We next reconstructed Z-stacked confocal microscopic images of starving cells, which confirmed that the LAMP1⁺ LC3⁻ tubules emanated from autolysosomal membranes. They appeared to give rise to LAMP1⁺ LC3⁻ vesicles by direct budding (Fig. 1e). Time-lapse microscopy revealed that tubule extension is a continuous and highly dynamic process with the distal portions of tubules extruding free vesicles (Fig. 1f and Supplementary Movie 2). We also used a photoactivatable GFP-tagged LAMP1 (PAGFP-LAMP1) for pulse-chase analysis of the autolysosomal membrane. After 4 h of starvation, individual autolysosomes were laser-activated and followed by time-lapse microscopy. Within 20 min, we observed tubule formation followed by budding of LAMP1⁺ vesicles (Fig. 1g and Supplementary Movie 3). Vesicle formation was not inhibited by the protein synthesis inhibitor cycloheximide (Supplementary Fig. 7).

When we tested for lysosomal properties, we found that the LAMP1⁺ tubules were not stained by the acid-dependent dye LysoTracker, despite strong staining of the autolysosomes (Fig. 2a). Furthermore, the lysosomal substrate DQ-BSA was degraded within the autolysosomes, but not the tubules (Fig. 2b). Thus, the newly formed tubules and vesicles lacked key biochemical characteristics of autolysosomes or lysosomes. We therefore preloaded starved cells with dextran, and found that it filled the autolysosomes but did not enter the tubules, confirming our observation from immuno-TEM

¹Laboratory of Immunology, National Institute of Allergy and Infectious Diseases, National Institutes of Health, Bethesda, Maryland 20892, USA. ²School of Life Science, Tsinghua University, Beijing 100084, China. ³State Key Laboratory of Biomembrane and Membrane Biotechnology, Beijing, 100084, China. ⁴Department of Cancer Biology, University of Massachusetts Medical School, Worcester, Massachusetts 01605, USA. ⁵Department of Cell Biology and Molecular Genetics, University of Maryland, College Park, Maryland 20742, USA. ⁶Cell Biology and Metabolism Program, National Institute of Child Health & Human Development, National Institutes of Health, Bethesda, Maryland 20892, USA. ⁷Department of Physiology, Universidad Austral de Chile, Valdivia 509-9200, Chile. ⁸Department of Biochemistry and Molecular Biology, Peking University Health Science Center, 38 Xueyuan Road, Beijing 100191, China. ⁹Department of Cell Biology, University Medical Center Utrecht, 3584CX Utrecht, The Netherlands.

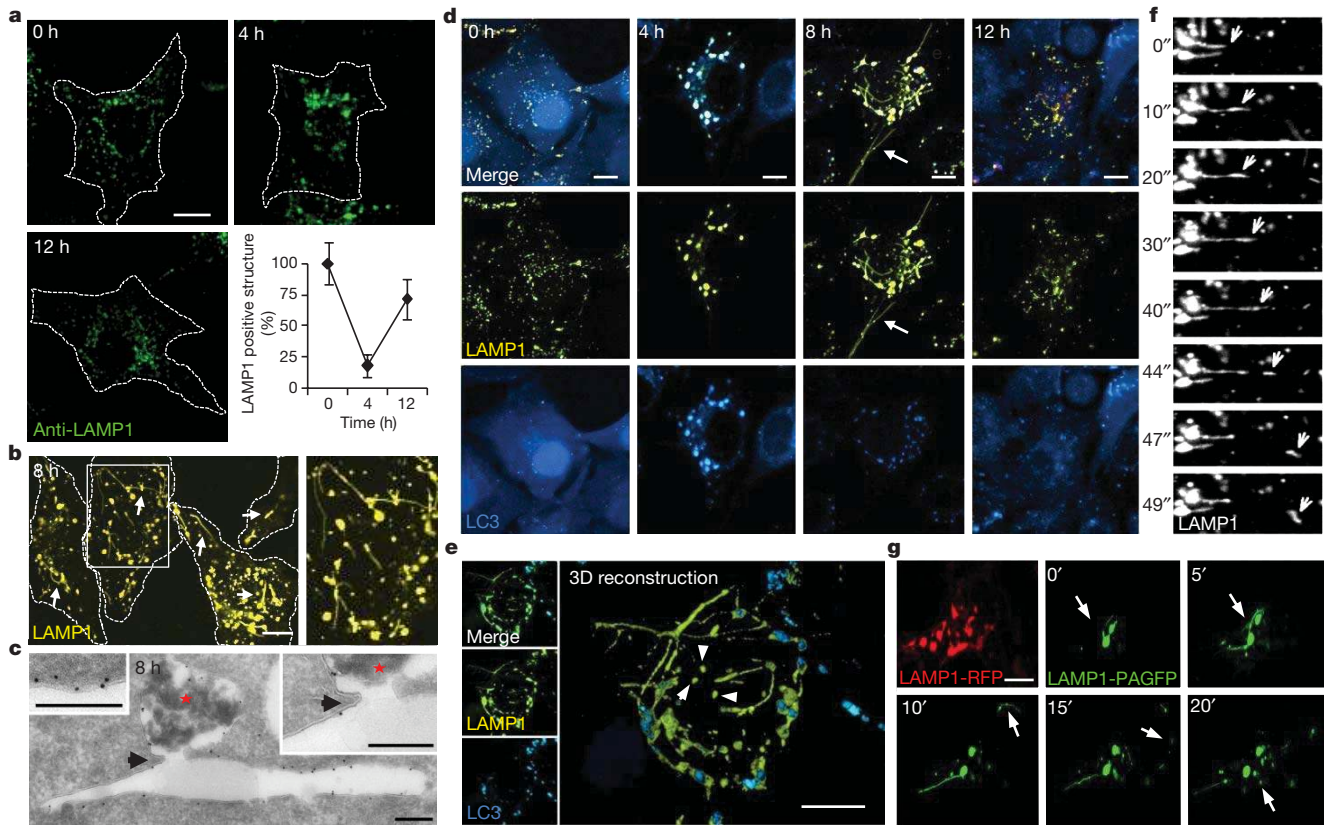


Figure 1 | Lysosome homeostasis during starvation. **a**, LAMP1⁺ lysosome size and quantity in NRK cells (dotted outline) starved for hours (h). Error bars show s.e.m. ($n = 3$). **b**, Starved NRK cells expressing LAMP1-YFP show tubules (arrows). Box is expanded on the right. **c**, Immuno-TEM (gold marks LAMP1) of starved NRK cells. Continuity (arrow) illustrated between autolysosome (red star) and tubule. **d**, LAMP1-YFP expressing NRK-LC3

cells as in **a**. Arrows show reformation tubules. **e**, Three-dimensional reconstruction of a cell from **d**. **f**, Time-lapse images (seconds) of starved LAMP1-YFP-expressing NRK cells. **g**, Time-lapse images (minutes) of starved LAMP1-PAGFP or LAMP1-RFP-expressing NRK cells after photo-activation. Scale bars, 5 μm .

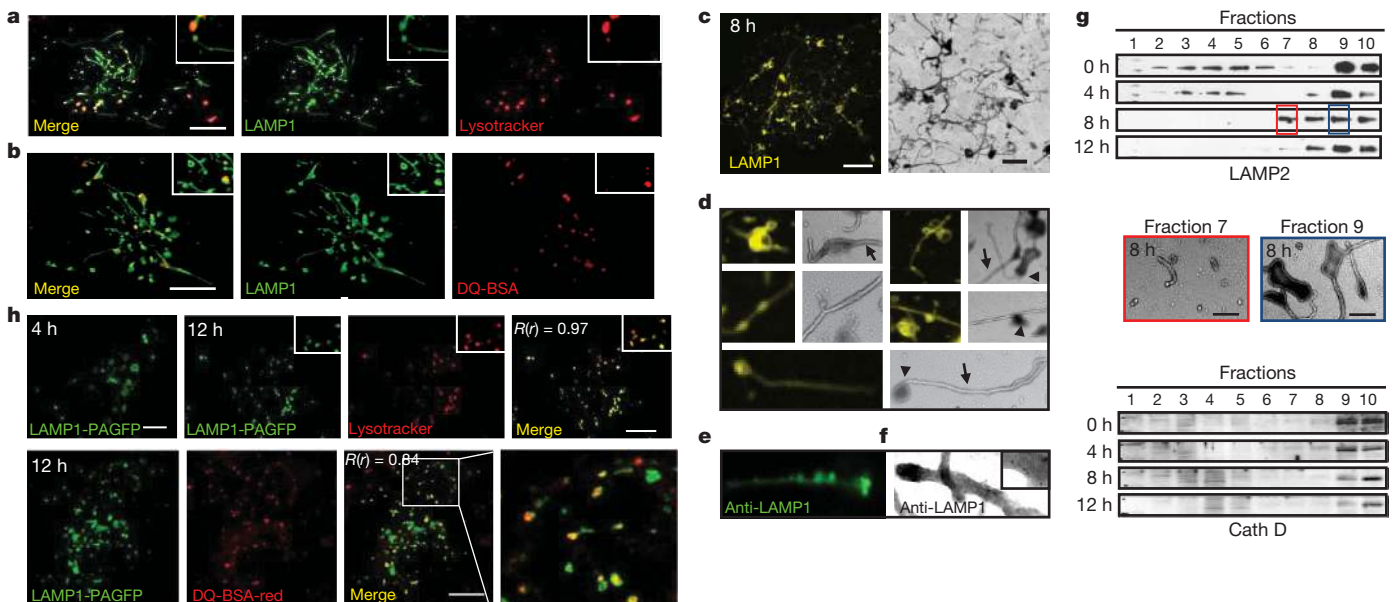


Figure 2 | Proto-lysosome formation and maturation. **a-c**, Starved LAMP1-YFP NRK cells stained with Lysotracker or DQ-BSA. **c**, Right, TEM of purified lysosomes. **d**, Magnification (4 \times) of images shown in **c**. Arrows indicate reformation tubules and arrowhead indicates autolysosome. **e, f**, Immunofluorescence (**e**) and immuno-EM (**f**) using LAMP1 antibody of cells shown in **c**. **g**, Density gradient fractions of NRK cells starved for times

shown and blotted for LAMP2 or Cathepsin D. Middle panel shows 8-h fractions 7 and 9 analysed by TEM. Fraction 10 is the gradient top. **h**, Starved LAMP1-PAGFP NRK cells were photo-activated (4 h) and imaged at 12 h with Lysotracker (upper) or DQ-BSA (lower). Boxes show enlargements. $R(r) =$ Pearson's coefficient. Scale bars, 5 μm .

that autolysosomal contents are withheld from the tubules (Supplementary Fig. 8).

We next used Optiprep (60% w/v iodixanol in H₂O) gradients to purify the autolysosomal fraction from starved NRK cells. This yielded an extensive tangle of autolysosomes and tubules whose morphology by TEM resembled tubules observed *in vivo* (Fig. 2c–f). The autolysosomal contents were clearly sequestered from the generally unfilled tubules (Fig. 2d). Using detailed gradient fractionation, we found that before starvation (time = 0 h), LAMP2 staining, lysosomal cathepsins D and B, and acid phosphatase activity were chiefly detected in mature lysosome fractions at the top of the gradient (fractions 9 and 10; Fig. 2g and Supplementary Fig. 9). After 4 h of starvation, when autophagosomes fuse to lysosomes, LC3 becomes transiently coincident with LAMP2 in fraction 9, biochemically confirming the evanescence of autolysosomes (Fig. 2g and Supplementary Fig. 9). Simultaneously, LAMP2 in fraction 10 is reduced, reflecting lysosome consumption during autophagy. At 8 h, as tubules and budding vesicles appear, two denser fractions (7 and 8) become LAMP2⁺ but not LC3⁺, and lack cathepsins or acid phosphatase (Fig. 2g and Supplementary Fig. 9). In fraction 7, TEM revealed mainly short tubules and vesicles, whereas fraction 9 contained autolysosomes extending tubules (Fig. 2g). These data reinforce the concept that reformation tubules and tubule-derived vesicles represent recycling of the lysosomal membrane components, but not of autolysosomal contents.

Co-localization analyses showed that LAMP1⁺ tubules and vesicles were not acidic after 8 h of starvation (Fig. 2a). However, by 12 h, the LAMP1⁺ vesicles became acidic (Supplementary Fig. 10), possibly maturing into functional lysosomes. We therefore visually tracked vesicles derived from PAGFP–LAMP1-labelled autolysosomes. Cells were starved for 4 h, PAGFP–LAMP1 was activated, and starvation was continued for a further 8 h, during which tubule-derived vesicles (smaller than autolysosomes) became acidic (Fig. 2h). Moreover, these vesicles also acquired the capacity to cleave DQ-BSA (Fig. 2h). Thus, the autolysosome-derived vesicles apparently mature into functionally active lysosomes and are henceforth referred to as proto-lysosomes.

Autophagy is generally held to be a constitutive process that is strongly induced during starvation^{1,6,7}. In agreement with recent findings^{8,9}, we observed that the number of autophagic cells is transient during starvation and peaks after 4 h but steadily decreases to almost none after 12 h (Fig. 3a, c and Supplementary Fig. 11). This attenuation of autophagy correlated with the initiation of autophagic lysosome reformation (ALR), hinting at a common coordinating mechanism. mTOR is a key governor of cell growth and metabolism that is rapidly inhibited during starvation, which triggers autophagy^{6,10}. We found that phosphorylation of the mTOR substrates S6 Kinase (S6K) and 4E-BP1 was inhibited after 2 h of starvation, but restored by 6 h and thereafter, indicating that mTOR signalling is reactivated despite ongoing starvation (Fig. 3b, c).

mTOR is activated by growth factors and nutrients, such as carbohydrates, amino acids and ATP¹⁰, and the chief role of autophagy during starvation is to provide nutrients by degrading cellular contents¹. We therefore tested whether intracellular nutrients generated by autophagy could stimulate mTOR signalling, and thereby provide a negative feedback signal to downregulate autophagy and trigger ALR. Knock-down of the autophagy essential gene *atg5* or *atg7* markedly inhibited the recovery of S6K phosphorylation (Fig. 3d and Supplementary Fig. 12). Reactivation of mTOR seems to trigger ALR, because adding the mTOR inhibitor rapamycin after 2 h of starvation also blocked S6K phosphorylation and ALR, resulting in enlarged autolysosomes persisting even after 10 h of starvation (Fig. 3e–g). Note that at the time of rapamycin addition, mTOR activity was already inhibited by starvation, so rapamycin was blocking mTOR reactivation. We also found, as shown previously¹¹, that knocking down mTOR increases autophagy but totally inhibits ALR, leaving giant autolysosomes which persist even after 12 h of starvation (Supplementary Fig. 13). mTOR was recently reported to localize to endosomes¹², so we examined its subcellular localization during starvation and found that a small fraction of mTOR colocalizes with LC3 after autolysosome formation. This indicates that mTOR might directly regulate ALR (Supplementary Fig. 14).

We further investigated the molecular requirements for ALR. First, we found that proto-lysosomes were closely associated with and

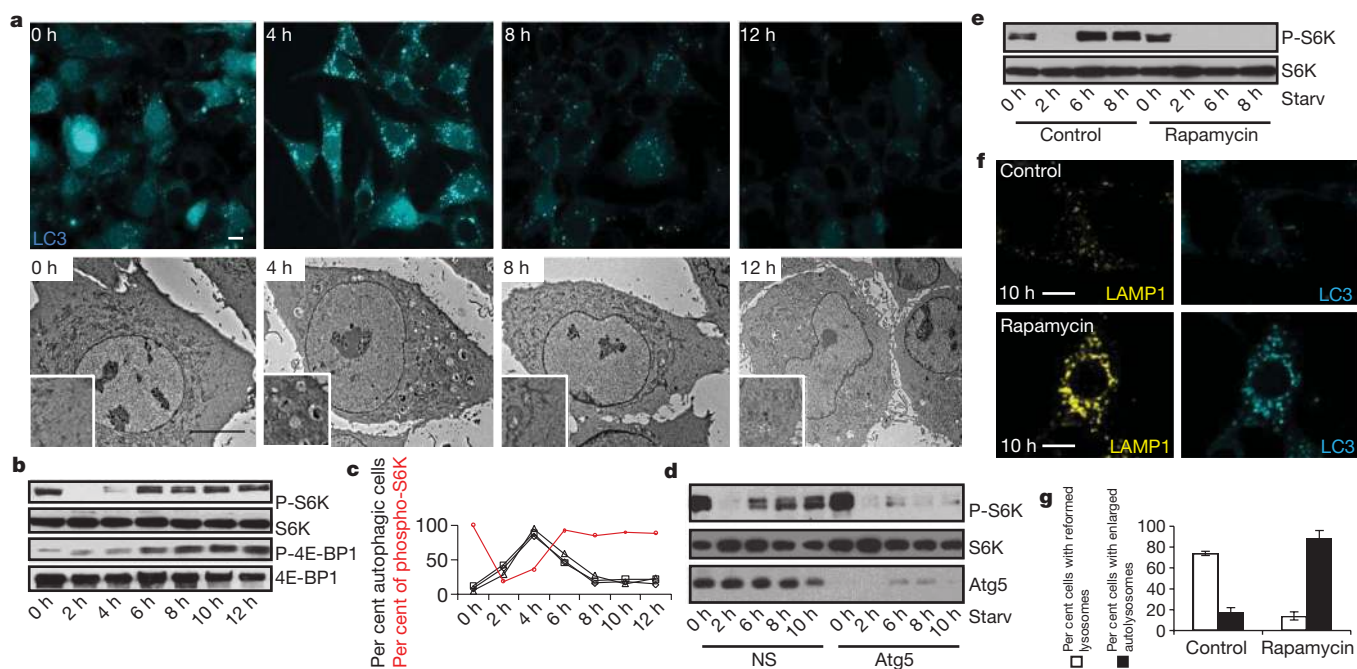


Figure 3 | Reactivation of mTOR inhibits autophagy and initiates lysosome reformation. **a**, TEM (bottom; scale bar, 5 μ m) and fluorescence (top; scale bar, 10 μ m) of NRK-LC3 cells starved for times shown with enlargements (boxes). **b**, **d**, Immunoblots of cells shown in **a** with indicated antibodies (**d**, after transfection with non-specific (NS) or *atg5* RNAi). **c**, Autophagy

(black lines show independent experiments) and phospho-S6K percentage (densitometry of data shown in **b**, red line). **e–g**, LAMP1–YFP NRK-LC3 cells starved for 2 h and then treated with 100 nM rapamycin for another 4 h (total, 6 h) or 6 h (total, 8 h) analysed by blotting (**e**) as in **b** or microscopy (**f**; scale bar, 5 μ m) with quantification (**g**). Error bars, s.e.m.; $n = 3$.

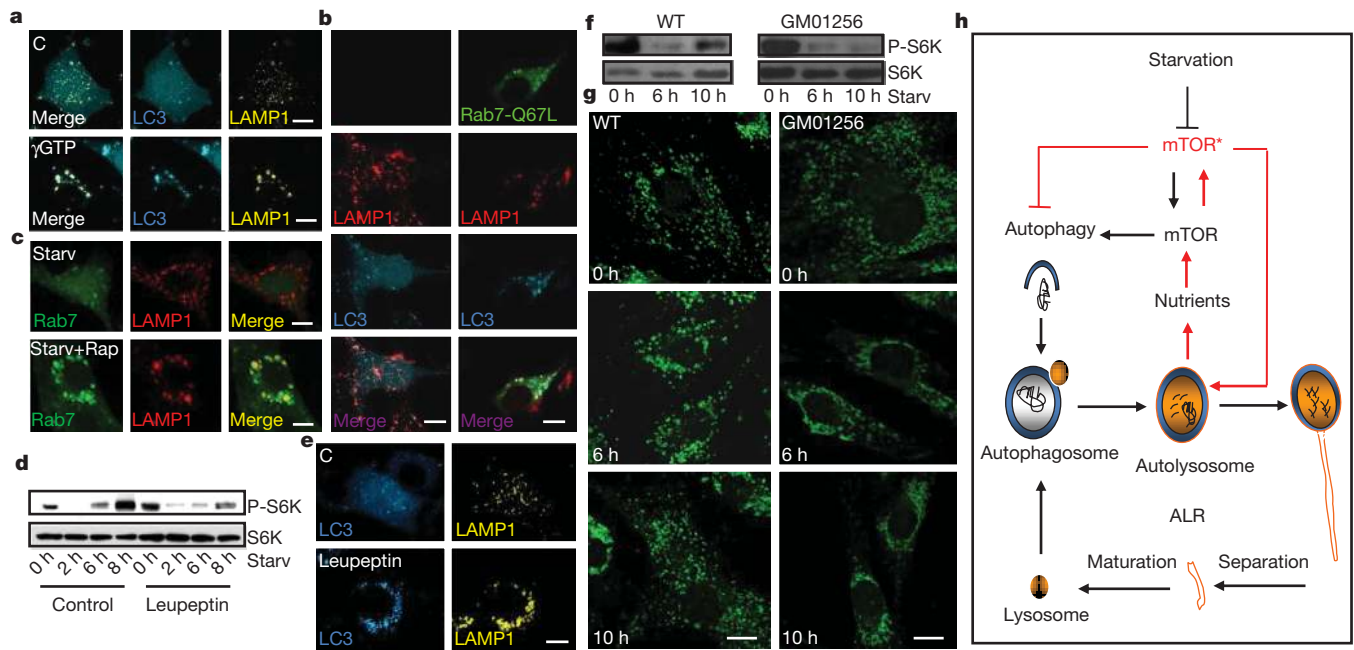


Figure 4 | Autophagic lysosome reformation. **a**, LAMP1/LC3 NRK cells were starved for 4 h and treated with GTP γ S for 6 h of further starvation. **b**, Rab7Q67L–GFP-transfected LC3–CFP/Lamp1–RFP NRK cells starved for 10 h. **c**, Rab7–CFP NRK cells starved for 2 h and treated with 100 nM rapamycin for 8 h of further starvation. **d**, LAMP1–YFP NRK-LC3 cells starved for times shown with 1 μ g ml $^{-1}$ leupeptin and blotted with indicated

decorate microtubules (Supplementary Fig. 15). Also, disruption of microtubules with nocodazole arrested ALR and induced giant persisting autolysosomes (Supplementary Fig. 15). Thus, microtubules are required for ALR, possibly providing a scaffold for the extrusion of reformation tubules. Second, we found that the small GTPase Rab7 is a key regulator of this process. Treating cells with GTP γ S, a non-hydrolysable analogue of GTP, completely inhibited ALR, leaving only enlarged autolysosomes (Fig. 4a). Rab7 resides on autolysosomes and mediates autophagosome–lysosome fusion³. We detected Rab7 in lysosomal fractions but not in proto-lysosome and tubule fractions after 8 or 12 h of starvation (Supplementary Fig. 16). We conjectured that Rab7 must dissociate from tubules before reformation can proceed. We therefore overexpressed constitutively active Rab7, which is permanently associated with the membrane, and found that ALR was abrogated, resulting in enlarged and long-lasting autolysosomes (Fig. 4b). Inhibition of ALR by rapamycin blocks dissociation of Rab7 from the distended autolysosomes it produced, indicating that mTOR might regulate ALR through Rab7 (Fig. 4c).

We also observed that inhibition of autolysosomal protein degradation by the lysosomal inhibitors leupeptin or E64/pepstatin A during starvation abolished reactivation of mTOR (Fig. 4e and Supplementary Fig. 17). Inhibition of lysosomal proteases also abrogated the attenuation of autophagy and ALR, resulting in enlarged and long-lasting autolysosomes (Fig. 4e). Significantly, fibroblasts derived from patients with the lysosome storage diseases (LSDs) Scheie syndrome (GM01256), Fabry disease (GM00636) and Aspartylglucosaminuria (GM02056) show impaired mTOR reactivation and defective lysosome reformation (Fig. 4f, g and Supplementary Figs 18, 19). The LAMP1 structures in leupeptin-treated cells or cells from patients with LSDs are slightly elongated compared to those from cells treated with rapamycin, possibly due to the accumulation of undegraded material in the autolysosome. Although we cannot exclude the possibility that altered pH or other defects contribute to aberrant ALR in cells from patients with LSDs, these observations are consistent with the conclusion that lysosomal degradative capability is required for ALR.

antibodies. **e**, Cells in **d** imaged. **f**, Fibroblast cells from patients with Scheie syndrome (GM01256) or healthy controls starved and blotted with indicated antibodies. **g**, Cells in **f** imaged. Lysosome size classified by Image-ProPlus (IPP) software. **h**, Provisional model of the autophagic lysosome reformation (ALR) cycle. Scale bars, 5 μ m.

Previous work has shown that autophagy leads to fusion of lysosomes and autophagosomes to form autolysosomes, but whether this restores a nutrient balance and how this affects lysosome homeostasis is not understood. We found that a large percentage of lysosomes are subsumed into autolysosomes at the peak of autophagy. However, we also observed that autophagy was eventually consummated and the normal complement of lysosomes was restored by an unknown mechanism. We have described a negative feedback mechanism that reverses autophagy and restores lysosome homeostasis, which we term autophagic lysosome reformation (ALR). The degradation of macromolecules and release of intracellular constituents following autophagy seems to trigger reactivation of mTOR, which inhibits autophagy and stimulates the recycling of proto-lysosomal membrane components via tubules and then vesicles that mature into new lysosomes (Fig. 4h). Genetic or chemical inhibition of lysosome function arrests ALR despite starvation. This feedback mechanism tightly couples nutritional status to the induction and cessation of autophagy. Thus, autophagy is self-regulated so that nutrient replenishment prevents excess autophagy, which could lead to autophagic cell death^{13–15}. As part of this cycle of lysosome consumption and restitution, ALR allows the cell to reuse a critical component that is required for further autophagy, the lysosomal membrane and associated proteins, in a time of scarce resources.

METHODS SUMMARY

NRK cells were cultured and maintained in DMEM medium with or without (starvation condition) 10% FBS and 2 mM L-glutamine. Cells were transfected using Amaxa nucleofection using solution T and program X-001, using 200 pmol RNAi or total 2 μ g DNA of expression plasmids prepared by standard molecular biology methods. Transfected cells were re-plated in LabTek chamber coverglasses (NUNC) grown overnight at 37 °C with 5% CO₂ in an open chamber (PeCon) for microscopy. Stains for lysosomal markers and LysoTracker were carried out using the manufacturers' recommended procedures. Images were digitally acquired by a Leica TCS SP5 confocal microsystem and analysed using instrument software and by the IMARIS package (Bitplane). For immuno-EM, cells were fixed in 4% formaldehyde in 0.1 M phosphate buffer (pH 7.4), and then in 4% formaldehyde. Ultrathin cryosectioning and immunogold labelling were as described¹⁶. For

lysosome isolation, we used a kit from Sigma-Aldrich. Cell fractionation and lysosome isolation were performed according to the manufacturer's instructions. Protein extraction procedures, gel electrophoresis, and immunoblotting were as described^{15,17}.

Full Methods and any associated references are available in the online version of the paper at www.nature.com/nature.

Received 27 July 2009; accepted 1 April 2010.

Published online 6 June 2010.

- Mizushima, N. Autophagy: process and function. *Genes Dev.* **21**, 2861–2873 (2007).
- Xie, Z. & Klionsky, D. J. Autophagosome formation: core machinery and adaptations. *Nature Cell Biol.* **9**, 1102–1109 (2007).
- Jager, S. *et al.* Role for Rab7 in maturation of late autophagic vacuoles. *J. Cell Sci.* **117**, 4837–4848 (2004).
- Jahreiss, L., Menzies, F. M. & Rubinsztein, D. C. The itinerary of autophagosomes: from peripheral formation to kiss-and-run fusion with lysosomes. *Traffic* **9**, 574–587 (2008).
- Kimura, S., Noda, T. & Yoshimori, T. Dissection of the autophagosome maturation process by a novel reporter protein, tandem fluorescent-tagged LC3. *Autophagy* **3**, 452–460 (2007).
- Scott, R. C., Schuldiner, O. & Neufeld, T. P. Role and regulation of starvation-induced autophagy in the *Drosophila* fat body. *Dev. Cell* **7**, 167–178 (2004).
- Wullschlegel, S., Loewith, R. & Hall, M. N. TOR signaling in growth and metabolism. *Cell* **124**, 471–484 (2006).
- Massey, A. C., Follenzi, A., Kiffin, R., Zhang, C. & Cuervo, A. M. Early cellular changes after blockage of chaperone-mediated autophagy. *Autophagy* **4**, 442–456 (2008).
- Mizushima, N. & Kuma, A. Autophagosomes in GFP-LC3 transgenic mice. *Methods Mol. Biol.* **445**, 119–124 (2008).
- Dennis, P. B. *et al.* Mammalian TOR: a homeostatic ATP sensor. *Science* **294**, 1102–1105 (2001).
- Ravikumar, B. *et al.* Inhibition of mTOR induces autophagy and reduces toxicity of polyglutamine expansions in fly and mouse models of Huntington disease. *Nature Genet.* **36**, 585–595 (2004).
- Sancak, Y. *et al.* The Rag GTPases bind raptor and mediate amino acid signaling to mTORC1. *Science* **320**, 1496–1501 (2008).
- Yu, L., Lenardo, M. J. & Baehrecke, E. H. Autophagy and caspases: a new cell death program. *Cell Cycle* **3**, 1124–1126 (2004).
- Yu, L., Strandberg, L. & Lenardo, M. J. The selectivity of autophagy and its role in cell death and survival. *Autophagy* **4**, 567–573 (2008).
- Yu, L. *et al.* Regulation of an ATG7-beclin 1 program of autophagic cell death by caspase-8. *Science* **304**, 1500–1502 (2004).
- Slot, J. W. & Geuze, H. J. Cryosectioning and immunolabeling. *Nature Protocols* **2**, 2480–2491 (2007).
- Bidère, N. *et al.* Casein kinase 1 α governs antigen-receptor-induced NF- κ B activation and human lymphoma cell survival. *Nature* **458**, 92–96 (2009).

Supplementary Information is linked to the online version of the paper at www.nature.com/nature.

Acknowledgements We thank the National Institute of Allergy and Infectious Diseases (NIAID) imaging core facility and Olympus China for technical support; O. Schwartz, J. Kabat, L. Koo, M. Czapiga (Bio-imaging facility (BIF), NIAID, NIH) and Q. Dong (Olympus China) for assistance with confocal microscopy and imaging processing; K. Nagashima and M. J. de la Cruz (NCI) for TEM analyses; J. Lippincott-Schwartz, H. Bernstein, and J. Bonifacino for helpful discussions; D. Yamamoto, G. Davis and H. Kramer for constructs and fly strains; and M. v. Peski and R. Szwed for assistance with the preparation of the EM figures. This research was supported by the Division of Intramural Research of the NIAID, NIH, Department of Health and Human Services and NIH Grant GM079431 to E.B., 973 program 2010CB833704, NSF grant 20091300700, and Tsinghua University grant 20091081391 to Y.L. J.K. is the recipient of VICI grant 918.56.611 of the Netherlands Organisation for Scientific Research (NWO).

Author Contributions L.Y. first observed lysosome reformation at the end of autophagy, autophagy dependent mTOR reactivation and performed the original characterization of the phenomenon. G.A.M. and D.W.H. made critical DNA constructs and designed the live imaging experiments. L.Z. performed the density gradient analyses. C.K.M. performed *Drosophila* experiments. V.O. performed immuno-TEM analyses. M.J.L. and L.Y. wrote the manuscript and J.P., Y.R., N.M., Y.Z., Z.L. and F.W. helped in the manuscript revision experiments. Most of the experiments were performed by L.Y. and were conceived by L.Y., E.H.B. and M.J.L. J.K. conceived and executed certain E.M. experiments. All authors wrote, discussed and revised the manuscript.

Author Information Reprints and permissions information is available at www.nature.com/reprints. The authors declare no competing financial interests. Readers are welcome to comment on the online version of this article at www.nature.com/nature. Correspondence and requests for materials should be addressed to M.J.L. (lenardo@nih.gov).

METHODS

Reagents and antibodies. LysoTracker-red, dextran-red (MW 10,000), DQ-BSA-red, Hoechst and DQ-ovalbumin-green were from Invitrogen. Leupeptin was from Millipore. Cycloheximide and anti-LAMP1 antibody were from Sigma-Aldrich. Anti-P-S6K, Anti-S6K, anti-S6K, anti-P-4E-BP, anti-4E-BP, anti-atg7 and anti-LC3 antibodies were from Cell Signaling Technology. Anti-AP-3 antibody was from Developmental Studies Hybridoma Bank, anti-Cath B antibody from Santa Cruz Biotechnology and anti-Cath D antibody from BD Bioscience. Western blots were performed as described¹⁴.

Cell culture and transfection. NRK cells were obtained from American Type Culture Condition (ATCC) and cultured in DMEM (Life Technologies) medium supplemented with 10% FBS (5% CO₂). Cells were transfected by Amaxa nucleofection using solution T and program X-001, using 200 pmol RNAi or total 2 µg DNA. Cells were then cultured in growth medium for further analysis. For two rounds of transfection, cells were transfected with 200 pmol RNAi, and 72 h after transfection cells were transfected again with 100 pmol RNAi and up to 2 µg DNA. Starvation medium was DMEM medium without the addition of serum and glutamine. HELA, C166, MRC-5, SH-SY5Y, MEF, OP9, Vero, HuH7, DF-1, ZF4, A6, HepG2, OMK, A549 and H4-II-E-C3 cell lines were obtained from ATCC and cultured according to the repository instructions.

Constructs. The human *spinster* construct was kindly provided by D. Yamamoto, Waseda University, Japan. LAMP1 and LC3 constructs with CFP, RFP, YFP, GFP or PAGFP tags were provided by J. Lippincott-Schwartz, NICHD, NIH. Rab7-GTP and Rab7 were provided by J. Bonifacino, NICHD, NIH. RNAi were synthesized by Invitrogen: mTOR, CAGCAGCTGGTACATGACAAGTACTTT; atg5, GGCATTATCCAATTGGCCTACTGTT.

Live cell imaging. Transfected cells were re-plated in Lab Tek Chambered coverglass (NUNC) the night before imaging, and cells were maintained at 37 °C with 5% CO₂ in a PeCon open chamber. Images were acquired by a Leica sp5 confocal microscope. Three-dimensional models were constructed by collecting images by Z-stack scanning at 0.5-µm intervals, and images were collapsed to construct 3D models by IMRIS (Bitplane). For fly experiments, third instar larvae expressing *tub-LAMP1-GFP* (control), or trans-heterozygous *spinster* mutant larvae expressing LAMP1-GFP (*tub-LAMP1-GFP; spinster*¹⁰⁴⁰³/*spinster*^{K09905}) were

starved in moist Petri dishes lacking food at 25 °C. The fat body was dissected and stained with Hoechst, and samples were imaged immediately without fixation on a Zeiss AxiovisionZ.1 microscope with fluorescence. The number of lysosomes was measured using Zeiss Automeasure software. Lysosomes were quantified in at least seven different larvae per time-point, in fat cells from one fat body per larva and two fields per fat body. Each field contained 3–4 cells. The number of lysosomes per time point was normalized to the average number of lysosomes in non-starved (0 h) larvae. Error bars indicate s.d.

Cell fractionation. We used a lysosome isolation kit from Sigma-Aldrich. Cell fractionation and lysosome isolation were performed according to the manufacturer's instructions.

Staining. Cells were washed with PBS, fixed in 2% paraformaldehyde for 10 min, and permeabilized in 0.2% Triton X-100 for 5 min. They were blocked with 10% FBS in PBS for 30 min, stained with 10 µg ml⁻¹ of rabbit anti-LAMP1 (Sigma-Aldrich) in blocking buffer for 1 h, and washed with PBS three times. Cells were then stained with fluorescein isothiocyanate-conjugated (FITC) anti-rabbit secondary antibody (Becton Dickinson) in PBS for 1 h and washed with PBS three times.

Electron microscopy. Cells were fixed in 3% glutaraldehyde in 0.1 M MOPS buffer (pH 7.0) for 8 h at room temperature, then in 3% glutaraldehyde/1% paraformaldehyde in 0.1 M MOPS buffer (pH 7.0) for 16 h at 4 °C. They were then post-fixed in 1% osmium tetroxide for 1 h, and embedded in Spurr's resin, sectioned, doubly stained with uranyl acetate and lead citrate, and analysed using a Zeiss EM 10 TEM.

Immuno-electron microscopy. LAMP-1-YFP NRK cells were starved for 8 h and then fixed for immuno-electron microscopy by adding freshly-prepared 4% formaldehyde in 0.1 M phosphate buffer (pH 7.4) to an equal volume of culture medium. After 10 min, the fixative was replaced for post-fixation in 4% formaldehyde at 4 °C overnight. Ultrathin cryosectioning and immunogold labelling were performed as described¹⁶. The LAMP-1-YFP construct was detected by using polyclonal rabbit anti-LAMP-1/LGP120 M3 at a dilution of 1:650. This antibody was a kind gift from I. Mellman (Genentech, San Francisco). The antibody was marked by protein A–10 nm gold particles (Cell Microscopy Center, Utrecht, The Netherlands).